

1 **Using computer vision to detect and segment fire behavior**
2 **classifications in UAS-captured images**

3

4

5

6 Brett L Lawrence ^{AB*}, +1-936-581-6833, brett@ravenenvironmental.com; Emerson de Lemmus ^C

7 ^A Stephen F. Austin State University, 1936 North St, Nacogdoches, Texas 75962, USA

8 ^B Raven Environmental Services, Inc., 6 Oak Bend Drive, Huntsville, Texas 77340, USA

9 ^C Independent Researcher

10 * Corresponding Author: lawrenceb3@jacks.sfasu.edu

11

12

13 This manuscript a non-peer reviewed preprint submitted to EarthArXiv. It has also been
14 submitted to scientific journal, and following peer-review will potentially undergo changes from
15 its preprint version.

16 **Abstract**

17 The widely adaptable capabilities of artificial intelligence, in particular deep learning and computer
18 vision has led to significant research output regarding fire and smoke detection. Previous studies
19 often focus on themes like early fire detection, increased operational awareness, and post-fire
20 assessment. To further test the capabilities of deep learning detection in these scenarios, we collected
21 and labeled a unique aerial image dataset that determined whether specific types of fire behavior
22 could be reliably detected in prescribed fire settings. Our 960 labeled images were sourced from over
23 20.97 hours of UAS video collected during prescribed fire operations covering a large region of
24 Texas and Louisiana, U.S.. National Wildfire Coordinating Group (NWCG) fire behavior
25 observations and descriptions served as a reference for determining fire behavior classes during
26 labeling. YOLOv8 models were trained on NWCG Rank 1-3 fire behavior descriptions in grassland,
27 shrubland, forested, and combined fire regimes within our study area. Models were first trained and
28 validated on isolated image objects of fire behavior, and then on segmenting fire behavior in their
29 original parent images. Models trained using isolated image objects of fire behavior consistently
30 performed at a mAP of 0.808 or higher, with combined fire regimes producing the best results (mAP
31 = 0.897). Most segmentation models performed relatively poorly, except for the forest regime model
32 at a box and mask mAP of 0.59 and 0.611, respectively. Our results indicate that classifying fire
33 behavior with computer vision is possible in most fire regimes and fuel models, whereas segmenting
34 fire behavior around background information is relatively difficult. However, it may be a manageable
35 task with enough data, and when models are developed for a specific fire regime. With an increasing
36 number of destructive wildfires and new challenges confronting fire managers, identifying how new
37 technologies can quickly assess wildfire situations can assist wildfire responder awareness. Our
38 conclusion is that levels of abstraction deeper than mere detection of smoke or fire are possible using
39 computer vision, and could make even more detailed fire monitoring possible.

40 **Keywords:** YOLO, computer vision, fire behavior, fire detection, UAS

41 **Introduction**

42 The rapid evolution of unmanned aerial systems (UAS) or vehicles (UAV) and their payload
43 capabilities has led to their increased integration into wildland and prescribed fire operations. Some
44 areas of developing use include fire suppression (Lattimer et al., 2023), aerial ignition (Beachly et al.,
45 2016; Lawrence et al., 2023), and real-time or post-fire monitoring (Moran et al., 2019). These
46 innovations are timely, with more severe fires and lengthening fire seasons requiring innovative
47 solutions to managing destructive wildfire events (Flannigan et al., 2013; Bowman et al., 2017;
48 Bowman et al., 2020).

49 UAS technologies show potential to strategically fit into the operational framework of this
50 challenging fire environment (Ambrosia and Wegener, 2009; Zajkowski et al., 2016). For example,
51 UAS technology proves to be relatively safe, inexpensive, and low complexity when compared to
52 their manned counterparts (Shamaoma et al., 2022; Keerthinathan et al., 2023). UAS-captured
53 information is also relatively fine resolution and temporally flexible when compared to space-borne
54 and airborne remote sensing methods (Muchiri and Kimathi 2016; Pádua et al., 2017). This makes
55 UAS platforms an excellent option for detailed, small spatial extent observations and active-fire
56 monitoring. In this study, we address the increasing interest in utilizing UAS vehicles in conjunction
57 with computer vision, an advanced branch of artificial intelligence, to improve and automate the
58 detection of fire, smoke, and other fire related phenomena (Rahman et al., 2021; Zhan et al., 2021;
59 Chen et al., 2022). Specifically, our aim is to further these developments by employing the latest
60 “You Only Look Once” (YOLO) detection algorithm to identify specific fire behavior descriptions as
61 defined by the National Wildland Coordinating Group (NWCG).

62 Machine learning (ML) and its associative subclasses, such as deep learning, are continually being
63 developed to provide fire detection and prediction services (Castelli et al., 2015; Hodges and
64 Lattimer 2019; Abid, 2021). The intersection of deep learning and computer vision is where
65 opportunities exist for automating the detection of fire phenomenon with a reconnaissance tool such
66 as UAVs. The YOLO deep learning architecture, known for its accurate and real-time detection
67 capabilities, is a prominent model family in this field. Various studies have already employed YOLO
68 algorithms for fire and smoke detection (Mukhiddinov et al., 2022; Zhao et al., 2022; Bahhar et al.,
69 2023). In several cases, lighter and less processing intensive versions of YOLO architectures have
70 achieved performance and speed suitable for real-time applications (Wang et al., 2021; Wang et al.,
71 2022*b*; Zheng et al., 2023). Speed improvements were achieved by replacing the CSPDarknet
72 backbone network with MobileNet, a lightweight convolutional neural network for mobile and
73 embedded devices.

74 Modern computer vision algorithms such as YOLOv8 enable both detection and segmentation tasks.
75 Detection involves identifying and locating objects within an image, often represented as traditional
76 bounding box labels. In contrast, segmentation goes a step further by partitioning an image into
77 multiple pixel clusters, or segments. In this study, we separately attempt both detection and
78 segmentation of fire behavior classes. Detection minimally identifies whether fire behavior can be
79 successfully classified, whereas segmentation demonstrates a model's ability to delineate separate
80 fire behavior objects within the context of an entire image. Smoke and flame are amorphous and
81 complex features, and to our knowledge, effort to automate the classification of fire behavior is
82 currently unaddressed. Furthermore, evidence suggests that high-resolution UAS images are well
83 suited for deep learning tasks such as segmentation compared to lower resolution remote sensing
84 images (Osco et al., 2023).

85 One challenge encountered in developing fire-detection models is the extensive time needed to label
86 images for training effective computer vision models. To address this, some researchers have
87 expedited the process of compiling new datasets by using techniques such as learning without
88 forgetting (Sathishkumar et al., 2023) or semi-supervised learning (Wang et al., 2022a). Our goal
89 was to provide a unique dataset of labeled fire behavior classes in UAS-captured images to support
90 continued fire modeling efforts. In addition to the need for large image datasets to train effective
91 models, there are also questions of standardization of labeling techniques. The approach can vary,
92 depending on the method of image acquisition and varying fire settings. One example includes
93 distinguishing between smoke and flame detection, and the context in which one or the other, or
94 both, should be targeted for detection. In some scenarios, such as satellite remote sensing, smoke
95 detection is prioritized as flames are typically not discernable, whereas both flames and smoke can be
96 observed and detected when using an UAS (Barmpoutis et al., 2020). Based on our experience, the
97 ability to detect both is influenced by factors such as landscape type, fire intensity, whether smoke is
98 occluding flames, and altitude of flight. Given that UAS vehicles enable low altitude, high resolution
99 observations, our approach in model development and dataset creation was to attempt detecting both
100 flames and smoke in our classifications.

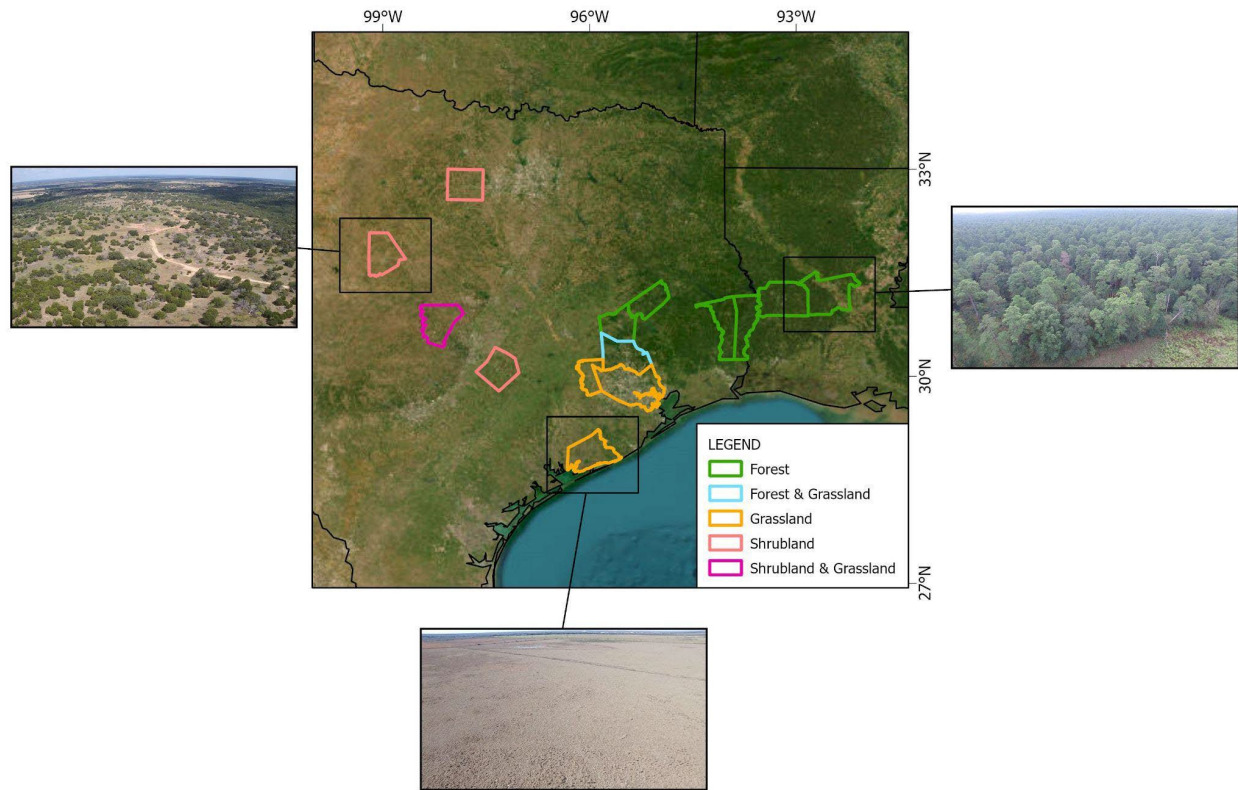
101 In summary, our goals for this study were outlined as follows: (1) Train separate YOLOv8 detection
102 models on isolated image objects of NWCG fire behavior for three different major fire regimes and
103 all the fire regimes combined; (2) train separate YOLOv8 segmentation models on entire parent
104 images for the same fire regimes; and (3) generate a unique and previously unavailable labeled image
105 dataset of fire behavior sourced from over five years of UAS-captured prescribed fire videos. For our
106 first two goals, we also generated validation metrics so we could compare model success in various
107 fire regimes and discuss the feasibility of computer vision for successfully classifying fire behavior.
108 Our intention is to determine whether more complex feature abstraction can be detected in fire

109 situations by computer vision, thereby providing even more detailed intelligence to personnel
110 responding to fire incidents. We feel these investigations are highly relevant, as wildland firefighters
111 internationally need new tools and technologies to address the increasingly complex fire environment
112 they are confronted with.

113 **Methods**

114 ***2.1 Study area***

115 Prescribed fire operations were conducted by Raven Environmental Services from years 2018-2023
116 throughout a regional area in Texas and Louisiana, U.S.. Dominant sub regional forest and land cover
117 types included Shortleaf Pine (*Pinus echinate*) and Loblolly Pine (*Pinus taeda*) forest in Walker,
118 Montgomery, and Trinity counties of Texas; Live Oak (*Quercus virginiana*) woodland and shrubland
119 in Parker, Brown, and Burnett counties of Texas; Loblolly Pine and Post Oak (*Quercus stellata*)
120 forest and woodland in Bastrop county Texas; Longleaf Pine (*Pinus palustris*) forest in Newton and
121 Jasper counties of Texas, and Vernon Parish of Louisiana; Coastal Prairie in Waller and Harris
122 counties of Texas; and one site-prep burn in Rapides Parish Louisiana. Described ecoregions
123 included Crosstimbers, Post Oak Savannah, Gulf Prairies and Marshes, Piney Woods ecoregions of
124 Texas (Griffith et al., 2007), and historically Longleaf Pine dominant areas of Louisiana.
125 Collectively, this made up a diverse geographic region of fuel types that was desirable when training
126 a computer vision model. When structuring images into major fire regimes for this study, we
127 generalized specific landscapes and vegetation types into three major categories: forest, grassland,
128 and shrubland (Figure 1).



129

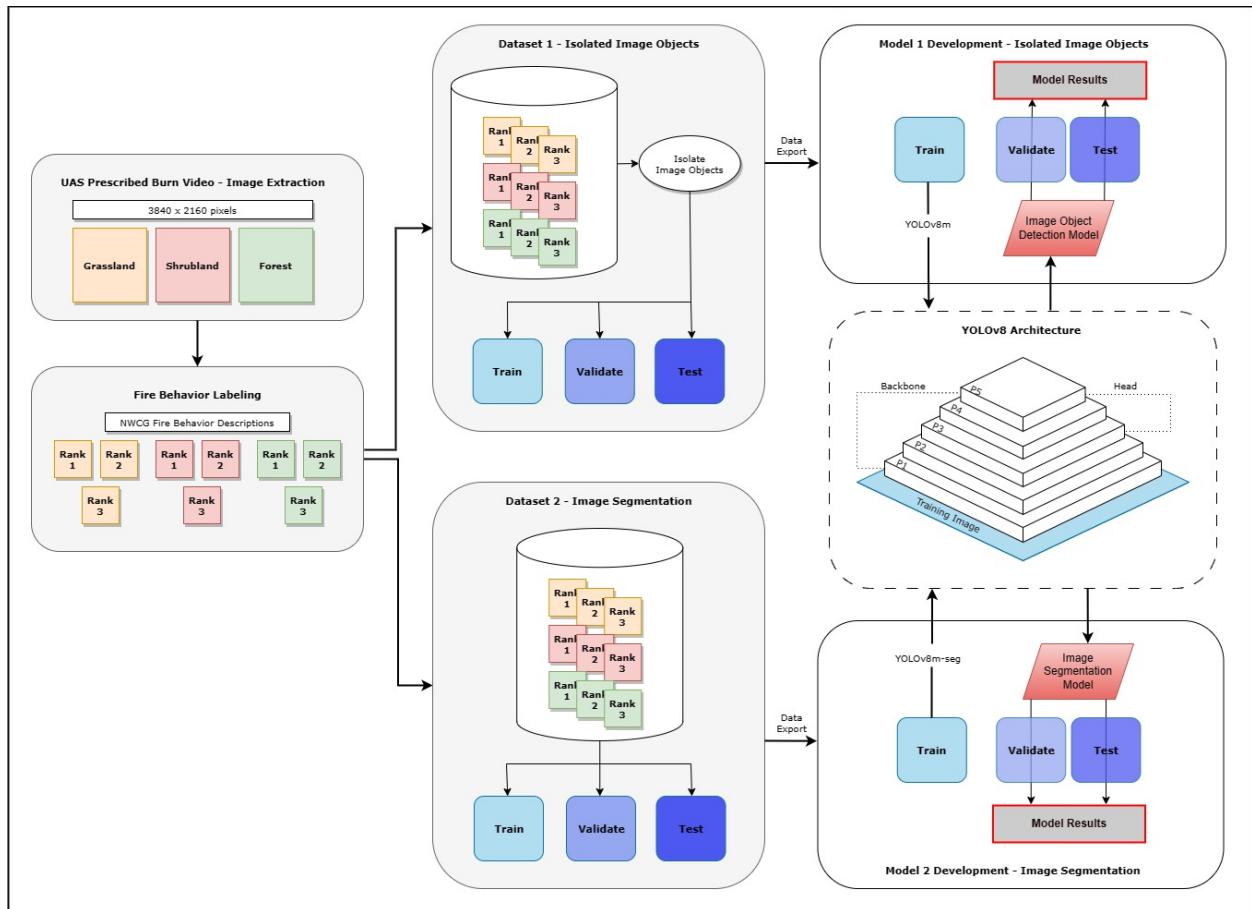
130 **Fig. 1.** The distribution of counties and parishes in Texas and Louisiana, U.S. where fire behavior images
131 were extracted from prescribed burn videos. Each location is symbolized to reflect the type of fire regime
132 images collected from that area.

133 **2.2 Image Dataset Description and Labeling**

134 **2.2.1 Image Extraction from Fire Videos**

135 Images were extracted from a total of 20.97 hrs of video captured during UAS aerial ignition flight
136 missions on 36 total prescribed burns. Videos were reviewed in Adobe Premiere Pro 2022 (Adobe
137 Inc., San Jose, California, US) and individual frames were captured at their original video resolution
138 of 3840 x 2160 pixels. Deliberate effort was made to diversify the image dataset by collecting a
139 balance of Rank 1-3 fire behavior classifications in each fire regime. Individual frames were also
140 captured in a multitude of luminosity settings, cloud cover, varying altitude, and gimbal angle.
141 Moreover, frames of different positioning of the fire (i.e. foreground, background, etc.), positioning

142 of smoke dispersal, prevailing wind and smoke travel relative to the UAS, the distance of the fire
 143 from the UAS, and the amount of fire and smoke in the field-of-view (FOV) all contribute to a
 144 dataset containing a variety of fire situations. Our image dataset development, labeling, and
 145 eventually model training workflow is visualized in Figure 2.



146

147 **Fig. 2.** Fire behavior dataset and model development workflow.

148 The dataset was subsequently imported into Roboflow (Roboflow, Des Moines, Iowa, US) for
 149 annotation. Utilizing the labeling tool powered by the Segment Anything Model (SAM), regions
 150 exhibiting varying fire behaviors were annotated in accordance with fire behavior descriptions and
 151 observations defined by the NWCG. SAM has recently been introduced as an excellent remote
 152 sensing image processing technique that harnesses zero-shot learning capabilities (Osco et al., 2023).

153 SAM was trained on the SA-1B dataset consisting of 1 billion masks and 11 million images, allowing
154 downstream users to transfer learning to new image datasets (Kirillov et al., 2023). For this work,
155 SAM’s efficiency in annotating complex phenomena such as fire behavior, typically a labor intensive
156 task, was significantly enhanced. The NWCG classifies fire behavior from Rank 1 (“smoldering”) to
157 Rank 6 (“erratic”). For example, Rank 1 fire behavior or “smoldering” consists of “no open flames in
158 surface fuels”, “white smoke”, and a “smoldering ground fire” (National Wildfire Coordinating
159 Group, 2021). Throughout the annotation process, descriptions and images provided by the NWCG
160 were consistently referenced to ensure accurate labeling of fire behavior types. Given that all images
161 originated from UAS video footage of prescribed fires, behaviors classified as Rank 4 (“torch/spot”)
162 were observed sporadically, while Rank 5 (“crowning”) and Rank 6 (“erratic”) were not observed.
163 Due to the necessity for balanced classes in computer vision model training , Rank 4 was excluded
164 from the annotation process to maintain dataset integrity, leaving Ranks 1 through 3 for subsequent
165 model training.

166 *2.2.1 Image Preprocessing, Augmentation, and Splits*

167 A total of 1,025 images were extracted from UAS prescribed burn videos for our study. Some of the
168 extracted frames were designated as null images or images that did not contain any of the targeted
169 fire behavior classes. Negative examples are important when training certain object detection or
170 classification models. They assist in the learning process by improving its ability to distinguish
171 between relevant and irrelevant information. Out of the initial collection, 960 images were annotated
172 into the final dataset and split into training, validation, and testing subsets (Table 1). Before their
173 inclusion into the dataset, these original 960 images were classified into distinct categories based on
174 the fire regimes they represent: grassland, shrubland, and forested areas (Table 1). This
175 categorization was followed by a series of preprocessing and augmentation steps to enhance the
176 dataset’s robustness and variability. Augmentation steps included cropping, saturation, and exposure

177 changes to original images, which provides the added benefit of artificially increasing the image
 178 dataset size. The entire curated image dataset has been made publicly available on Roboflow
 179 Universe, an open-source platform dedicated to sharing computer vision datasets (Fire Behavior,
 180 2024). This initiative aims to facilitate further research and advancements in the field of fire behavior
 181 analysis using computer vision.

182 **Table. 1.** Original image dataset sizes and the size of training, validation, and testing splits after
 183 preprocessing and augmentation.

Dataset	Original Images	Image Splits after Augmentation		
		Training	Validation	Testing
All – Isolated Image Objects	960	9585	279	243
All – Instance Segmentation	960	3555	141	92
Grassland – Isolated Image Objects	264	3470	121	63
Grassland – Instance Segmentation	264	985	45	22
Shrubland – Isolated Image Objects	354	3470	101	128
Shrubland – Instance Segmentation	354	1340	48	38

Forest – Isolated Image Objects	364	3095	83	65
Forest – Instance Segmentation	364	1365	56	35

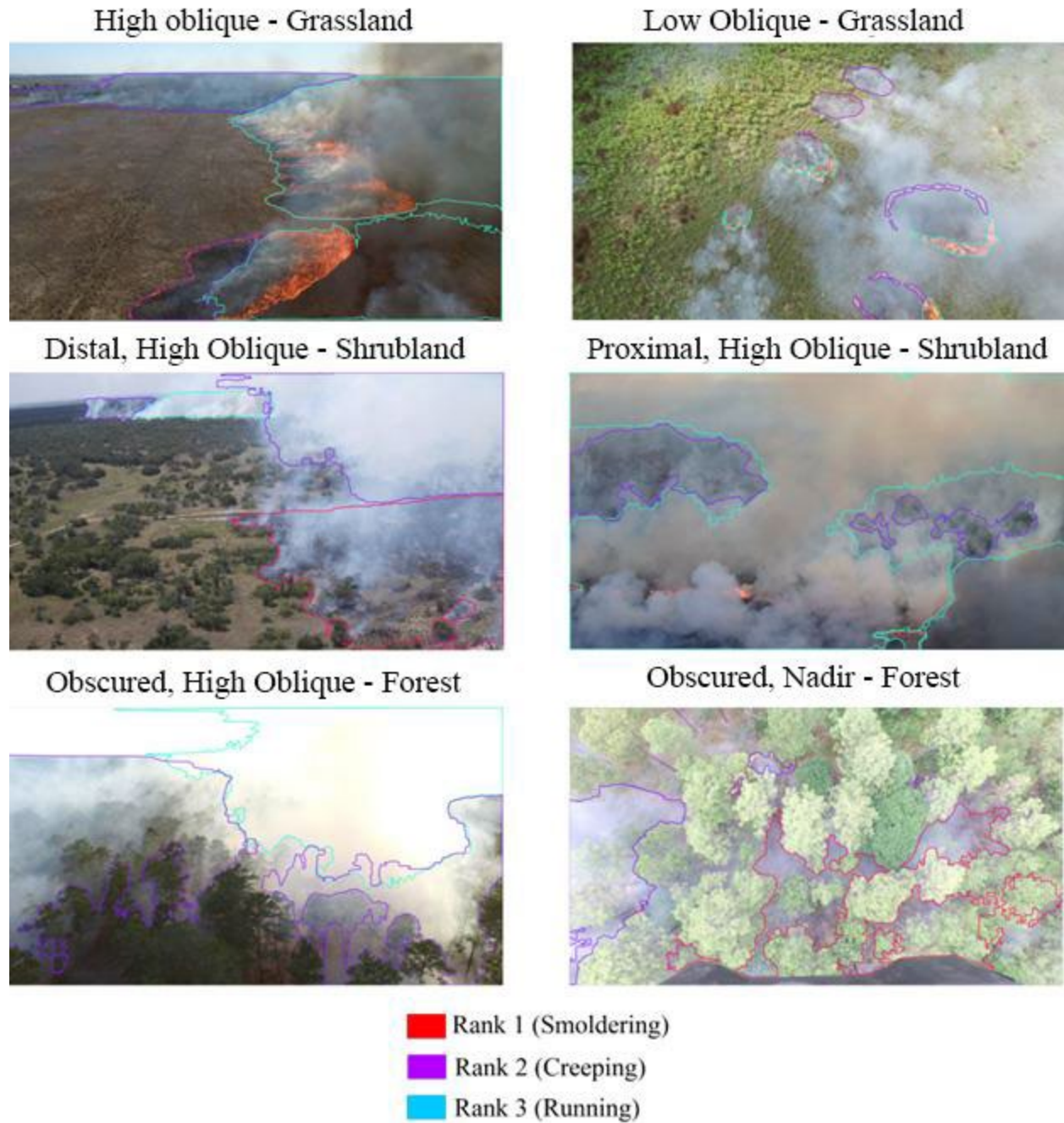
184

185 *2.2.3 Unique Labeling Scenarios*

186 Labeling was an iterative process because of the variety of fire situations and settings. This
187 necessitated careful consideration of how to standardize the labeling methodology. We list some
188 prominent examples here, and how we addressed them. For the grassland fire regime, dot ignition
189 sites could arguably be categorized as Rank 2 fire behavior during early ignition, but eventually
190 develop into Rank 3 on the downwind side as they radiate outwardly (Figure 2). Determining when
191 to begin dividing grassland fires into multiple fire behavior classifications was usually
192 straightforward, although not always. Additionally, grassland fires frequently presented visible
193 flames and smoke that could be labeled together. This was manageable at high oblique and horizontal
194 camera perspectives, but less so at low oblique or nadir perspectives. In the latter scenarios, the
195 smoke's organization relative to the flame source was complex, scattered, and sometimes disjunct.
196 We chose to label only flames in some low oblique or nadir perspectives because this might be the
197 most helpful to a potential end-user.

198 In situations where the UAS was a considerable distance from the fire's progression, flames might
199 only be visible in the foreground or not at all. This was true of shrubland and forest fire regimes,
200 where trees and vegetation often occlude or block the flame front. This could result in a mosaic of
201 smoke and/or flame features within one image (Figure 2). For example, the foreground of a
202 shrubland fire might have Rank 2 flames and smoke, and the background has Rank 2 and 3 smoke

203 only. High-oblique or horizontal shots often contained two or all three fire behavior ranks. Where to
204 delineate the transition from one to another was not always straightforward and could potentially
205 vary between different labelers. We continually reference our NWCG fire descriptions to provide
206 clarification in these situations. A challenge unique to forested regime labeling was strongly
207 occluded smoke in both oblique and nadir gimbal angles. We made an effort to be consistent when
208 labeling smoke in these scenarios (Figure 2).



209

210 **Fig. 3.** Examples of fire behavior labeling in all three fire regimes. Images of high oblique and low
211 oblique grassland fires demonstrate how developing spot fires can consist of multiple types of fire
212 behavior. Flames were often visible and labeled in grassland fires, but smoke could be difficult to label at
213 nadir or close to nadir gimbal angles. High oblique gimbal angles of shrubland fires when the UAS was

214 distal or proximal to the fire front presented situations with multiple types of fire behavior in one image.
215 Forested settings could be difficult to label because of smoke occluding tall trees.

216 ***2.3 Model Selection and Training***

217 YOLO deep learning architecture was used to train and develop our fire behavior classification
218 model. YOLO is known for its fast detection times and suitability for potential real-time applications
219 (Redmon et al., 2016). The YOLO family has undergone several version improvements since its
220 introduction as YOLOv3. Our model training was conducted in Google Colaboratory or Colab
221 (Bisong 2019) using the latest version, Ultralytics YOLOv8 (Jocher et al., 2023; Ultralytics, 2023b).
222 Google Colab provides cloud-based and open-source computing services for managing the large
223 processing requirements needed for model training. We used Python 3 runtime type with a NVIDIA
224 T4 GPU. Training was performed using 100 epochs, and an input resolution of 640 x 640 pixels.
225 Medium sized model options YOLOv8m-cls and YOLOv8m-seg were used to train the classification
226 and segmentation models respectively because of their balance of accuracy and training time.

227 ***2.4 Model Validation***

228 Model validation was performed using the “val” mode, which introduces the trained models to a new
229 set of images not used during training. Validation metrics included precision, recall, mean average
230 precision (mAP), and F1-Score with their values determined as follows:

231

$$\text{mAP} = \frac{\sum AP}{N(\text{Class})} \quad (1)$$

232

$$\text{Precision} = \frac{TP}{(TP+FP)} \quad (2)$$

$$\text{Recall} = \frac{TP}{(TP+FN)} \quad (3)$$

$$\text{F1 Score} = 2 \times \frac{(\text{Precision} \times \text{Recall})}{(\text{Precision} + \text{Recall})} \quad (4)$$

233

234 Model validation metrics were used to assess and compare model performance between our
 235 classification and image segmentation model. Testing data predictions were made last, and
 236 represented a real-world example of model deployment.

237 **Results**

238 *3.1 Isolated Image Object Detection*

239 For all fire regimes and combined regimes, YOLOv8 models trained using isolated image objects
 240 performed at a mAP of 0.808 or higher for all fire behavior classes (Table 2). Combined fire regimes
 241 performed the best for all classes at a mAP of 0.897 and F1-Score of 0.84 at a 0.494 confidence
 242 interval. Individual fire behavior classes typically performed better for the combined fire regime
 243 model, except for Rank 1 behavior, which performed best in the forest regime model. The lowest
 244 performing individual class was Rank 2 fire behavior for the forest regime at an average precision of
 245 0.605. The combined regimes and forest regime discontinued training at 69 and 83 epochs
 246 respectively because of stalled learning for several epochs.

247 **Table. 2.** Validation results for detection of isolated image objects of fire behavior in grassland,
 248 shrubland, forested, and combined fire regimes.

Dataset	Class	Precision	Recall	mAP@50	F1-Score
Combined	All	0.83	0.842	0.897	

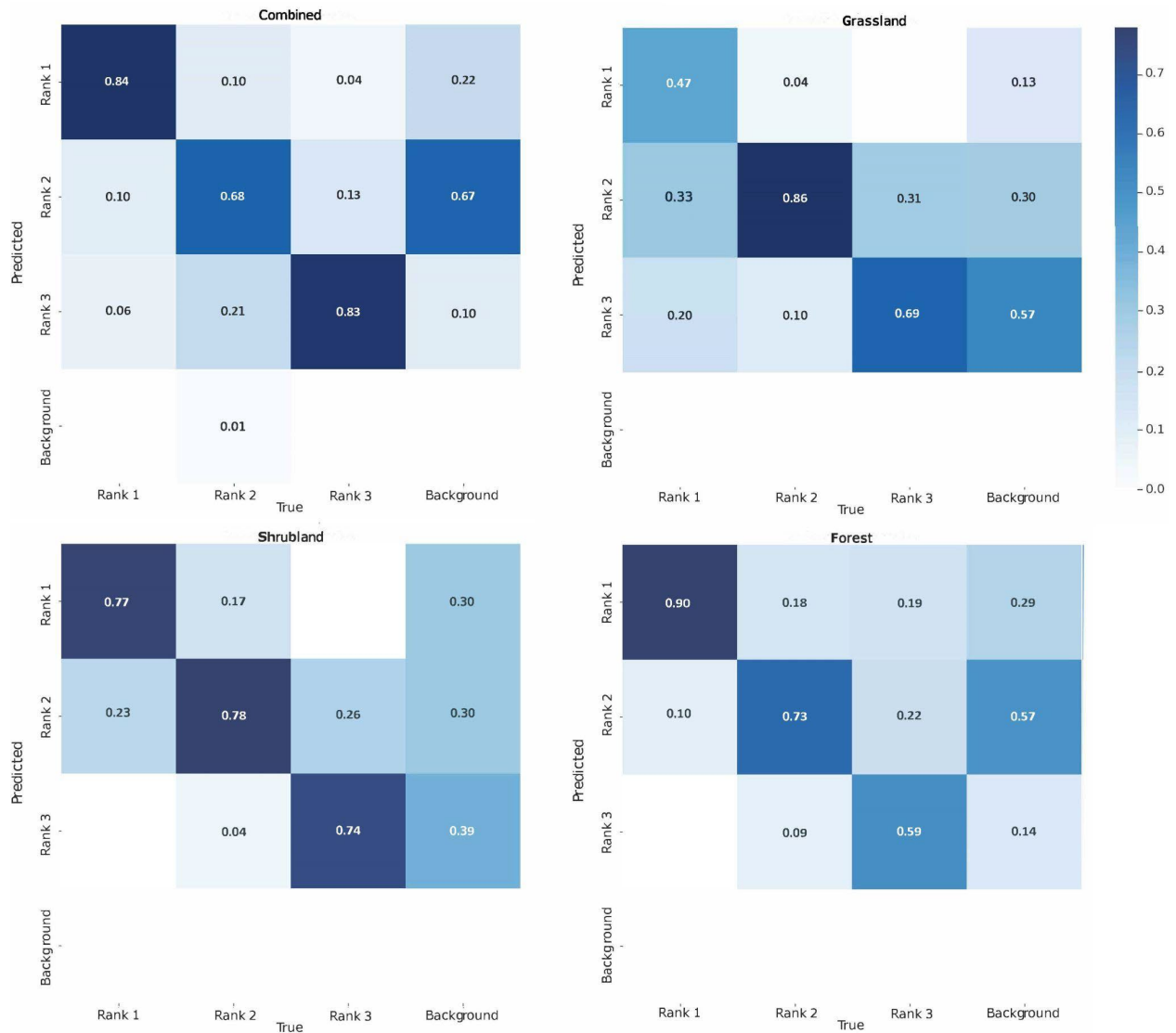
	Rank 1	0.872	0.877	0.912	0.84 @ 0.494
	Rank 2	0.822	0.824	0.879	
	Rank 3	0.798	0.827	0.902	
Grassland	All	0.818	0.696	0.814	0.74 @ 0.804
	Rank 1	0.839	0.533	0.784	
	Rank 2	0.822	0.868	0.86	
	Rank 3	0.792	0.686	0.798	
Shrubland	All	0.733	0.874	0.867	0.80 @ 0.337
	Rank 1	0.736	0.903	0.865	
	Rank 2	0.731	0.848	0.843	
	Rank 3	0.731	0.87	0.894	
Forest	All	0.729	0.808	0.808	0.72 @ 0.514
	Rank 1	0.857	0.92	0.926	
	Rank 2	0.377	0.883	0.605	
	Rank 3	0.952	0.621	0.892	

249

250 Normalized confusion matrix results for all four models demonstrate 0.73 or greater prediction
 251 accuracy of fire behavior classifications, with some exceptions (Figure 3). These include Rank 2 for
 252 the combined fire regimes, Rank 1 & 3 for grassland, and Rank 3 for forest. The only instance of less
 253 than 0.5 prediction accuracy was for Rank 1 fire behavior detection in grassland areas. Interclass
 254 prediction inaccuracies for all models were less than 0.26, except for grassland areas where over
 255 predictions of Rank 2 in cases of Rank 1 (0.33) and Rank 3 (0.31) were relatively frequent.

256 It is important to note that when interpreting a normalized YOLOv8 confusion matrix, the instances
 257 of predictions for each class (Rank 1- 3) versus true background is the false positive rate per class.
 258 This is the right-most column of the confusion matrix, and the sum of all classes is always one
 259 because they have been normalized. In this way, they are not a visualization of the number of false

260 positives – that number per class might be very low – but their values are instead the number of false
 261 positives relative to other classes. For example, when considering our model trained using data for
 262 combined fire regimes, the amount of false positives was much higher for Rank 2 fire behavior (0.67)
 263 than Rank 1 (0.22) or Rank 3 (0.10).



264
 265 **Fig. 4.** Normalized confusion matrix results for detection of isolated image objects of fire behavior in
 266 grassland, shrubland, forested, and combined fire regimes.

267 **3.2 Segmentation**

268 YOLOv8 segmentation of fire behavior in original parent images resulted in relatively low
 269 performance when compared to isolated image object counterparts. The highest mAP for all classes
 270 was accomplished with the forest regime dataset and resulted in a box mAP of 0.590 and mask mAP
 271 of 0.611 (Table 3). The forest regime model also produced the highest F1-Score of 0.64 at a
 272 confidence interval of 0.637. The next highest box and mask mAP for all classes was 0.343 and
 273 0.290 in the case of the grassland segmentation model. Contrary to isolated image objects, the
 274 combined fire regimes model's average precision per class underperformed several of the regime
 275 specific models. For example, the forest segmentation model outperformed for all classes in the case
 276 of both box and mask, and grassland out performed in Rank 2 & 3 for both, too. The shrubland
 277 segmentation model performed the worst for all three metrics; average precision per class, mAP, and
 278 F1-Score. It also discontinued training at 77 epochs because of stalled learning. Compared to
 279 detection models using isolated image objects, recall was disparately lower than precision across all
 280 segmentation models. Average box and mask precision for all four segmentation models was 0.52
 281 and 0.55, whereas average box and mask recall was 0.36 and 0.33, respectively.

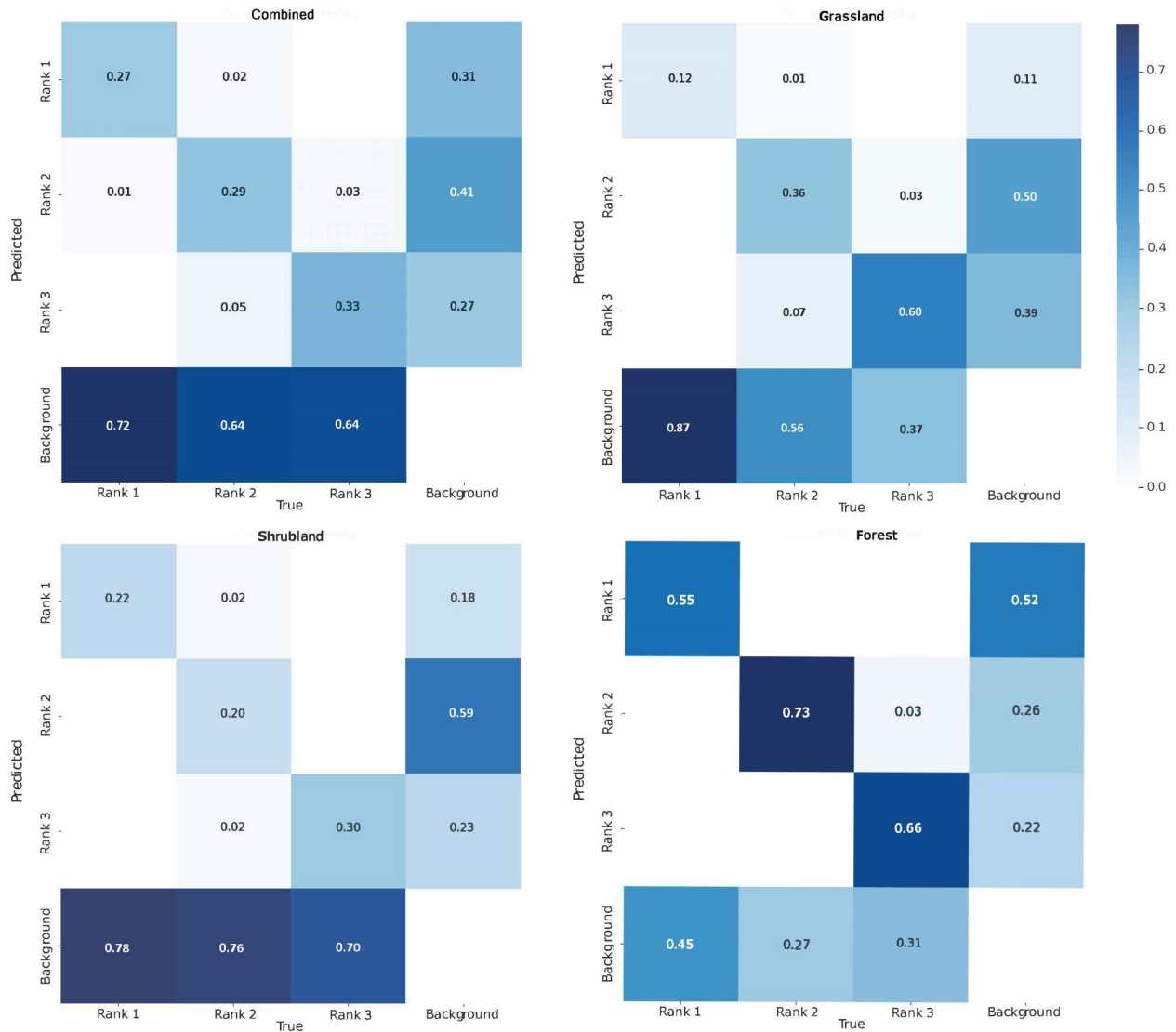
282 **Table. 3.** Validation results from segmentation of fire behavior in parent images of grassland, shrubland,
 283 forested, and combined fire regimes.

Dataset	Class	Box				Mask			
		Precision	Recall	mAP@50	F1-Score	Precision	Recall	mAP@50	F1-Score
Combined	All	0.431	0.314	0.302	0.37 @ 0.135	0.467	0.267	0.288	0.34 @ 0.490
	Rank 1	0.431	0.295	0.267		0.41	0.232	0.245	
	Rank 2	0.459	0.339	0.327		0.539	0.289	0.299	
	Rank 3	0.403	0.307	0.313		0.454	0.28	0.32	
Grassland	All	0.545	0.316	0.343	0.38 @	0.442	0.273	0.29	0.32 @
	Rank 1	0.434	0.125	0.113	0.539	0.216	0.0625	0.0705	0.538

	Rank 2	0.644	0.31	0.379		0.616	0.298	0.342	
	Rank 3	0.557	0.514	0.537		0.493	0.457	0.459	
Shrubland	All	0.447	0.229	0.202	0.31 @ 0.294	0.475	0.24	0.2	0.32 @ 0.304
	Rank 1	0.385	0.188	0.162		0.324	0.156	0.132	
	Rank 2	0.42	0.196	0.164		0.476	0.217	0.162	
	Rank 3	0.537	0.304	0.28		0.624	0.348	0.305	
Forest	All	0.666	0.599	0.59	0.62 @ 0.648	0.8	0.547	0.611	0.64 @ 0.637
	Rank 1	0.58	0.414	0.436		0.833	0.425	0.505	
	Rank 2	0.585	0.727	0.618		0.746	0.636	0.656	
	Rank 3	0.834	0.656	0.717		0.822	0.578	0.673	

284

285 Confusion matrix results for segmentation models demonstrated a significant number of errors in the
 286 form of underpredicting fire behavior for background (Figure 4). The only exception was the forest
 287 regime model, which managed to keep false background predictions under 0.5. The shrubland
 288 regime's lack of validation performance was reinforced in the confusion matrix results. Under
 289 prediction of fire behavior was significant for all classes (>0.70). The grassland segmentation model
 290 demonstrated more mixed interclass accuracy, with Rank 3 fire behavior being predicted moderately
 291 (0.6) and Rank 1 fire behavior predicted poorly (0.12). The combined fire regimes, while poor
 292 performing, were relatively balanced amongst classes and ranged from 0.27-0.33 prediction
 293 accuracy. A significant outcome was the small amount of interclass prediction errors. The largest
 294 amount of error was found when the grassland regime model was mistaking Rank 2 for Rank 3 fire
 295 behavior (0.07). Overall, background prediction errors were significant for all models except for the
 296 forest regime, whereas interclass prediction errors were minimal.



297

298 **Fig. 5.** Normalized confusion matrix results for segmentation of fire behavior in parent images of

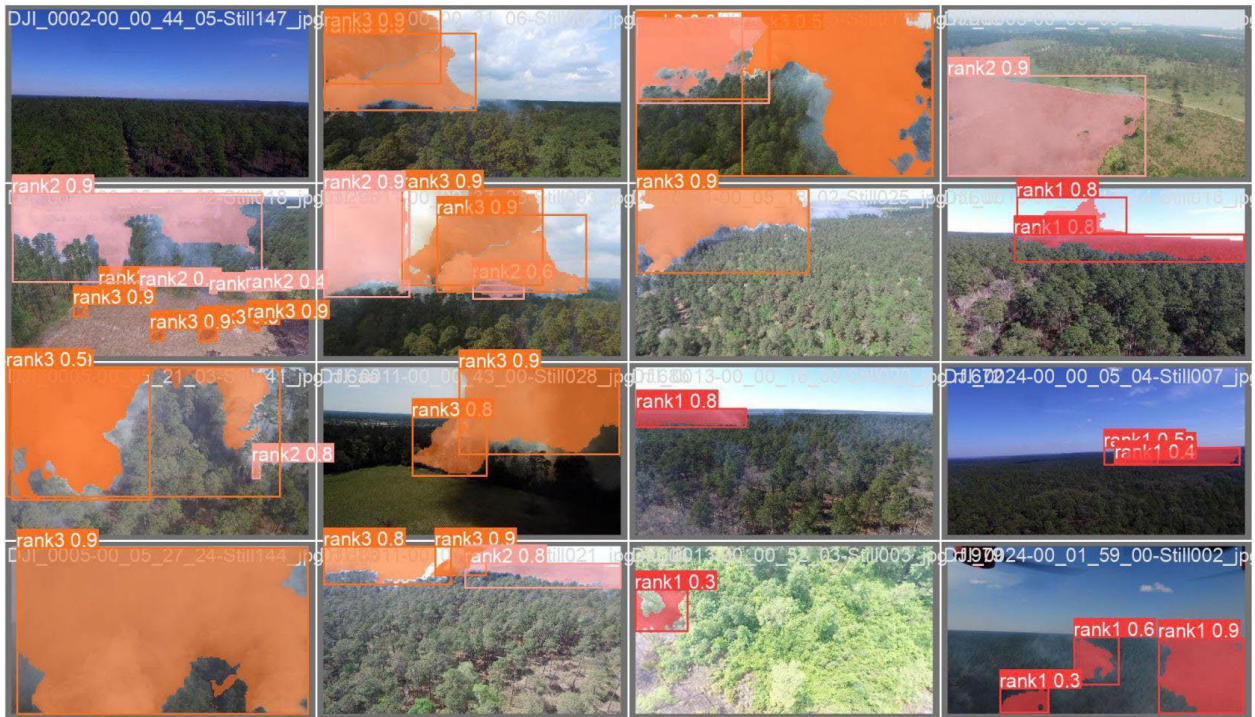
299 grassland, shrubland, forested, and combined fire regimes.

300 We also provide some examples of images labels versus box and mask predictions during the forest

301 regime segmentation model validation (Figure 6).



(a)



(b)

302

303 **Fig. 6.** Examples of (a) images labels and (b) predictions made during validation of our forest

304 segmentation model.

305

306 **Discussion**

307 *1.1 Interpretation of results*

308 Assessing fire situations quickly and accurately is an important requirement for fire managers
309 responding to wildfire situations or conducting prescribed fire operations. An understanding of
310 general classifications of on-scene fire behavior can immediately inform fire managers about the type
311 of situation they are dealing with and the appropriate response. We focused on (1) Training separate
312 YOLOv8 detection models on isolated image objects of NWCG fire behavior for three different
313 major fire regimes and all the fire regimes combined; (2) training separate YOLOv8 segmentation
314 models on entire parent images for the same fire regimes; and (3) generating a unique and previously
315 unavailable labeled image dataset of fire behavior sourced from over five years of UAS-captured
316 prescribed fire videos.

317 When analyzing isolated image objects of fire behavior, YOLO detection models reasonably
318 classified NWCG Rank 1-3 fire behavior in all our fire regimes ($mAP > 0.6$, $\bar{x} = 0.85$). While there
319 were some examples of classes within fire regimes that performed relatively poorly, the overall
320 results suggest that fire behavior is a visual phenomenon that can be trained and reliably detected
321 using computer vision methods. Furthermore, combining datasets and training a detection model
322 from images in all fire regimes resulted in increased model performance. This suggests that when
323 excluding background information the type of fire regime is not necessarily important when
324 classifying fire behavior with computer vision.

325 Model performance reduced significantly when training segmentation models on fire behavior with
326 parent images. The main explanation for this drop in performance in all four models was low recall,
327 or instances of missing fire behavior objects. Meanwhile, precision metrics were relatively high

328 compared to recall for all our segmentation models. This is also evidenced by normalized confusion
329 matrices for segmentation models, with instances of interclass errors being low but underpredicted
330 fire behavior being high for all classes (Figure 4). Ultralytics attributes low recall to the need for
331 improved feature extraction or lack of data (Ultralytics, 2023a). High-performing computer vision
332 models are often trained with image datasets on the scale of thousands to millions of labeled images,
333 so our lack of recall performance is likely attributable to our relatively small datasets. Unfortunately,
334 labeled image datasets of fire behavior are not readily available, and generating new data is time-
335 intensive. Despite this, our forest regime segmentation model still generated results of a potentially
336 deployable model.

337 Our conclusion is that fire behavior is a detectable phenomenon using computer vision, but making
338 accurate detections in a variety of scenarios is either difficult or requires more labeled image data for
339 some fire regimes. Moreover, fire behavior classification and masking within those regimes can be
340 variable because of circumstances unique to each fire regime described in our labeling methodology.
341 For example, Rank 3 fire behavior was predicted with reasonable accuracy by the grassland
342 segmentation model. One possible explanation is because flames are consistently visible in grassland
343 settings, and our labeling of flames allowed for an outlier in class performance.

344 Given this information, one of our most significant findings is that our results indicate computer
345 vision models are better developed for a specific fire regime, rather than several simultaneously. The
346 strongest indicator of this is the reduced performance in the combined fire regimes segmentation
347 model compared to the forest regime. Despite using around a third the amount of labeled images, the
348 forest regime model still outperformed its combined regime counterpart.. It is possible that
349 differences in feature extraction amongst fire regimes led to a diversity of scenes that negatively
350 impacted performance.

351 ***1.2 Future Considerations***

352 A more clearly defined standard for labeling fire behavior could benefit the continued development
353 of computer vision modeling of fire behavior in different fire regimes. Creating a standardized
354 system might lead to complementary datasets, helping with the issue of data availability and the time
355 intensiveness of labeling. For our work, data size was a limiting factor for segmentation model
356 performance in most fire regimes.

357 UAS platforms are making a strong foray into the operational framework of fire management
358 agencies, but their continued rapid evolution poses several challenges. Much of the work on UAS
359 vehicles is experimental, and their impact is usually constrained by their small-scale capabilities.
360 Furthermore, the presence of UAS vehicles in wildland fire airspace could arguably inhibit, or even
361 endanger, some of the manned flight operations that will always be necessary during wildfire
362 response. Managing interagency communication, understanding regulatory requirements, and
363 creating protocols for UAS response and where they fit in the larger operational effort are all
364 important challenges for UAS operators in fire. Examples of large unmanned vehicle deployment for
365 fire monitoring (Hall et al., 2008) and the use of edge-device computing (Fouda et al., 2023) both
366 demonstrate the operational possibilities of large and small UAS monitoring of fire. It is probable
367 that fire behavior detection could serve as an additional feature extraction tool during these types of
368 efforts.

369 **Conclusions**

Our study demonstrated that YOLOv8 computer vision modeling is capable of successfully detecting and classifying NWCG fire behavior descriptions. Our images were sourced from low-altitude UAS flights during prescribed burn operations and focused on relatively low-severity fire behavior (Rank 1-3). Furthermore, we have provided an open-sourced dataset for future modeling efforts. Model

precision, or successful detection of different classes of fire behavior, was high for different major fire regimes and all of them combined when training YOLO models on isolated image objects. Model precision remained acceptable when training YOLO segmentation models, but the introduction of background information around image objects led to a drastic reduction in recall and performance for all models but forested areas. For the forest regime, the segmentation model performed well enough to serve as a potentially useful model for real-time deployment, and minimally demonstrated that fire behavior can be segmented reliably in some circumstances using our methods. Our results suggest that future modeling efforts might be more successful if they are developed for a specific fire regime. This is especially important, considering the lack of data available and the time-intensiveness of developing new datasets. Lack of datasets consisting of several thousand labeled images was most likely the primary reason for low segmentation model performance. Overall, our study has demonstrated that in addition to smoke and flame detection, computer vision technologies can extract and identify even more nuanced fire phenomena. This development represents a step towards several opportunities available for leveraging deep learning, computer vision technology for advanced fire monitoring purposes.

370 **Declarations**

371 **Ethics approval and consent to participate:** Not applicable

372 **Consent for publication:** Not applicable

373 **Availability of data and material:** The labeled image dataset of combined fire regimes is available
374 at: <https://app.roboflow.com/raven-environmental-services/fire-behavior/9>

375 **Competing interests:** The authors declare that they have no competing interests.

376 **Funding:** This research received no external funding.

377 **Authors' contributions:** BL: conceptualization, data curation, formal analysis, methodology,
378 validation, writing - original draft, and writing - review and editing. EdL: formal analysis,
379 methodology, validation, and writing -review and editing.

380 **Acknowledgements:** The authors acknowledge the private landowners and public land management
381 agencies that approved our use of video acquired during prescribed burn operations. They include the
382 Texas National Guard, Texas Parks and Wildlife Division, and Cooks Branch Conservancy. The
383 author also thanks Dr. Brian Oswald and Dr. David Kulhavy for providing helpful discussion on how
384 to improve the study.

385 **References**

- 386 1. Abid, F., 2021. A Survey of Machine Learning Algorithms Based Forest Fires Prediction and
387 Detection Systems. *Fire Technol* 57, 559–590. <https://doi.org/10.1007/s10694-020-01056-z>
- 388 2. Ambrosia, V.G., Wegener, S.S., 2009. Unmanned Airborne Platforms For Disaster Remote
389 Sensing Support, in: Peter, P.-G. (Ed.), *Geoscience and Remote Sensing*. InTech.
390 <https://doi.org/10.5772/8302>
- 391 3. Bahhar, C., Ksibi, A., Ayadi, M., Jamjoom, M.M., Ullah, Z., Soufiene, B.O., Sakli, H., 2023.
392 Wildfire and Smoke Detection Using Staged YOLO Model and Ensemble CNN. *Electronics*
393 12, 228. <https://doi.org/10.3390/electronics12010228>
- 394 4. Barmpoutis, P., Stathaki, T., Dimitropoulos, K., Grammalidis, N., 2020. Early Fire Detection
395 Based on Aerial 360-Degree Sensors, Deep Convolution Neural Networks and Exploitation
396 of Fire Dynamic Textures. *Remote Sensing* 12, 3177. <https://doi.org/10.3390/rs12193177>
- 397 5. Beachly, E., Higgins, J., Laney, C., Elbaum, S., Detweiler, C., Allen, C., Twidwell, D., 2017.
398 A micro-UAS to Start Prescribed Fires, in: Kulić, D., Nakamura, Y., Khatib, O., Venture, G.
399 (Eds.), *2016 International Symposium on Experimental Robotics*, Springer Proceedings in

- 400 Advanced Robotics. Springer International Publishing, Cham, pp. 12–24.
401 https://doi.org/10.1007/978-3-319-50115-4_2
- 402 6. Bisong, E., 2019. Google Colaboratory, in: Building Machine Learning and Deep Learning
403 Models on Google Cloud Platform. Apress, Berkeley, CA, pp. 59–64.
404 https://doi.org/10.1007/978-1-4842-4470-8_7
- 405 7. Bowman, D.M.J.S., Kolden, C.A., Abatzoglou, J.T., Johnston, F.H., Van Der Werf, G.R.,
406 Flannigan, M., 2020. Vegetation fires in the Anthropocene. *Nat Rev Earth Environ* 1, 500–
407 515. <https://doi.org/10.1038/s43017-020-0085-3>
- 408 8. Bowman, D.M.J.S., Williamson, G.J., Abatzoglou, J.T., Kolden, C.A., Cochrane, M.A.,
409 Smith, A.M.S., 2017. Human exposure and sensitivity to globally extreme wildfire events.
410 *Nat Ecol Evol* 1, 0058. <https://doi.org/10.1038/s41559-016-0058>
- 411 9. Castelli, M., Vanneschi, L., Popovič, A., 2015. Predicting Burned Areas of Forest Fires: an
412 Artificial Intelligence Approach. *fire ecol* 11, 106–118.
413 <https://doi.org/10.4996/fireecology.1101106>
- 414 10. Chen, X., Hopkins, B., Wang, H., O'Neill, L., Afghah, F., Razi, A., Fulé, P., Coen, J.,
415 Rowell, E., Watts, A., 2022. Wildland Fire Detection and Monitoring Using a Drone-
416 Collected RGB/IR Image Dataset. *IEEE Access* 10, 121301–121317.
417 <https://doi.org/10.1109/ACCESS.2022.3222805>
- 418 11. Fire Behavior Image Dataset [WWW Document], 2024. Roboflow Universe. URL
419 <https://app.roboflow.com/raven-environmental-services/fire-behavior/9> (accessed 1.24.24).
- 420 12. Flannigan, M., Cantin, A.S., De Groot, W.J., Wotton, M., Newbery, A., Gowman, L.M.,
421 2013. Global wildland fire season severity in the 21st century. *Forest Ecology and*
422 *Management* 294, 54–61. <https://doi.org/10.1016/j.foreco.2012.10.022>

- 423 13. Fouda, M.M., Sakib, S., Fadlullah, Z.M., Nasser, N., Guizani, M., 2022. A Lightweight
424 Hierarchical AI Model for UAV-Enabled Edge Computing with Forest-Fire Detection Use-
425 Case. *IEEE Network* 36, 38–45. <https://doi.org/10.1109/MNET.003.2100325>
- 426 14. Griffith, G., Bryce, S., Omernik, J., Rogers, A., 2007. Ecoregions of Texas. Texas
427 Commission on Environmental Quality.
- 428 15. Hall, P., Cobleigh, B., Buoni, G., Howell, K., 2008. Operational Experience with Long
429 Duration Wildfire Mapping: UAS Missions Over the Western United States, in: *AUVSI*
430 *Unmanned Systems North America 2008*. National Oceanic and Atmospheric Administration
431 & NASA Dryden Flight Research Center, San Diego, CA.
- 432 16. Hodges, J.L., Lattimer, B.Y., 2019. Wildland Fire Spread Modeling Using Convolutional
433 Neural Networks. *Fire Technol* 55, 2115–2142. <https://doi.org/10.1007/s10694-019-00846-4>
- 434 17. Jocher, G., Chaurasia, A., & Qiu, J. (2023). YOLO by Ultralytics (Version 8.0.0) [Computer
435 software]. <https://github.com/ultralytics/ultralytics>
- 436 18. Keerthinathan, P., Amarasingam, N., Hamilton, G., Gonzalez, F., 2023. Exploring unmanned
437 aerial systems operations in wildfire management: data types, processing algorithms and
438 navigation. *International Journal of Remote Sensing* 44, 5628–5685.
439 <https://doi.org/10.1080/01431161.2023.2249604>
- 440 19. Kirillov, A., Mintun, E., Ravi, N., Mao, H., Rolland, C., Gustafson, L., Xiao, T., Whitehead,
441 S., Berg, A.C., Lo, W.-Y., Dollár, P., Girshick, R., 2023. Segment Anything.
- 442 20. Lattimer, B.Y., Huang, X., Delichatsios, M.A., Levendis, Y.A., Kochersberger, K., Manzello,
443 S., Frank, P., Jones, T., Salvador, J., Delgado, C., Angelats, E., Parés, M.E., Martín, D.,
444 McAllister, S., Suzuki, S., 2023. Use of Unmanned Aerial Systems in Outdoor Firefighting.
445 *Fire Technol*. <https://doi.org/10.1007/s10694-023-01437-0>

- 446 21. Lawrence, B.L., Mundorff, K., Keith, E., 2023. The impact of UAS aerial ignition on
447 prescribed fire: a case study in multiple ecoregions of Texas and Louisiana. *fire ecol* 19, 11.
448 <https://doi.org/10.1186/s42408-023-00170-x>
- 449 22. Moran, C.J., Seielstad, C.A., Cunningham, M.R., Hoff, V., Parsons, R.A., Queen, Ll.,
450 Sauerbrey, K., Wallace, T., 2019. Deriving Fire Behavior Metrics from UAS Imagery. *Fire* 2,
451 36. <https://doi.org/10.3390/fire2020036>
- 452 23. Muchiri, N., Kimathi, S., 2016. A Review of Applications and Potential Applications of
453 UAV, in: 2016 Annual Conference on Sustainable Research and Innovation. Presented at the
454 Proceedings of the Sustainable Research and Innovation Conference.
- 455 24. Mukhiddinov, M., Abdusalomov, A.B., Cho, J., 2022. A Wildfire Smoke Detection System
456 Using Unmanned Aerial Vehicle Images Based on the Optimized YOLOv5. *Sensors* 22,
457 9384. <https://doi.org/10.3390/s22239384>
- 458 25. National Wildfire Coordinating Group, 2021. Fire Behavior Observations/Descriptions
459 [WWW Document]. Fire Behavior Observations. URL
460 <https://www.nwccg.gov/publications/pms437/cffdrs/fire-behavior-observations> (accessed
461 11.13.23).
- 462 26. Osco, L.P., Wu, Q., de Lemos, E.L., Gonçalves, W.N., Ramos, A.P.M., Li, J., Junior, J.M.,
463 2023. The Segment Anything Model (SAM) for Remote Sensing Applications: From Zero to
464 One Shot.
- 465 27. Pádua, L., Vanko, J., Hruška, J., Adão, T., Sousa, J.J., Peres, E., Morais, R., 2017. UAS,
466 sensors, and data processing in agroforestry: a review towards practical applications.
467 *International Journal of Remote Sensing* 38, 2349–2391.
468 <https://doi.org/10.1080/01431161.2017.1297548>

- 469 28. Rahman, E.U., Khan, M.A., Algarni, F., Zhang, Y., Irfan Uddin, M., Ullah, I., Ahmad, H.I.,
470 2021. Computer Vision-Based Wildfire Smoke Detection Using UAVs. *Mathematical*
471 *Problems in Engineering* 2021, 1–9. <https://doi.org/10.1155/2021/9977939>
- 472 29. Redmon, J., Divvala, S., Girshick, R., Farhadi, A., 2016. You Only Look Once: Unified,
473 Real-Time Object Detection, in: 2016 IEEE Conference on Computer Vision and Pattern
474 Recognition (CVPR). Presented at the 2016 IEEE Conference on Computer Vision and
475 Pattern Recognition (CVPR), IEEE, Las Vegas, NV, USA, pp. 779–788.
476 <https://doi.org/10.1109/CVPR.2016.91>
- 477 30. Sathishkumar, V.E., Cho, J., Subramanian, M., Naren, O.S., 2023. Forest fire and smoke
478 detection using deep learning-based learning without forgetting. *fire ecol* 19, 9.
479 <https://doi.org/10.1186/s42408-022-00165-0>
- 480 31. Shamaoma, H., Chirwa, P.W., Ramoelo, A., Hudak, A.T., Syampungani, S., 2022. The
481 Application of UASs in Forest Management and Monitoring: Challenges and Opportunities
482 for Use in the Miombo Woodland. *Forests* 13, 1812. <https://doi.org/10.3390/f13111812>
- 483 32. Ultralytics YOLOv8 Docs [WWW Document], 2023a. Performance Metrics Deep Dive.
484 URL <https://docs.ultralytics.com/guides/yolo-performance-metrics/> (accessed 1.24.24).
- 485 33. Ultralytics YOLOv8 Docs [WWW Document], 2023b. The New Frontier of Vision AI. URL
486 <https://docs.ultralytics.com/> (accessed 11.13.23).
- 487 34. Wang, J., Fan, X., Yang, X., Tjahjadi, T., Wang, Y., 2022a. Semi-Supervised Learning for
488 Forest Fire Segmentation Using UAV Imagery. *Forests* 13, 1573.
489 <https://doi.org/10.3390/f13101573>
- 490 35. Wang, S., Zhao, J., Ta, N., Zhao, X., Xiao, M., Wei, H., 2021. A real-time deep learning
491 forest fire monitoring algorithm based on an improved Pruned + KD model. *J Real-Time*
492 *Image Proc* 18, 2319–2329. <https://doi.org/10.1007/s11554-021-01124-9>

- 493 36. Wang, Y., Hua, C., Ding, W., Wu, R., 2022*b*. Real-time detection of flame and smoke using
494 an improved YOLOv4 network. *SIViP* 16, 1109–1116. [https://doi.org/10.1007/s11760-021-](https://doi.org/10.1007/s11760-021-02060-8)
495 02060-8
- 496 37. Zhao, L., Zhi, L., Zhao, C., Zheng, W., 2022. Fire-YOLO: A Small Target Object Detection
497 Method for Fire Inspection. *Sustainability* 14, 4930. <https://doi.org/10.3390/su14094930>
- 498 38. Zajkowski, T.J., Dickinson, M.B., Hiers, J.K., Holley, W., Williams, B.W., Paxton, A.,
499 Martinez, O., Walker, G.W., 2016. Evaluation and use of remotely piloted aircraft systems
500 for operations and research – RxCADRE 2012. *Int. J. Wildland Fire* 25, 114.
501 <https://doi.org/10.1071/WF14176>
- 502 39. Zhan, J., Hu, Y., Cai, W., Zhou, G., Li, L., 2021. PDAM–STPNNet: A Small Target
503 Detection Approach for Wildland Fire Smoke through Remote Sensing Images. *Symmetry*
504 13, 2260. <https://doi.org/10.3390/sym13122260>
- 505 40. Zheng, H., Duan, J., Dong, Y., Liu, Y., 2023. Real-time fire detection algorithms running on
506 small embedded devices based on MobileNetV3 and YOLOv4. *fire ecol* 19, 31.
507 <https://doi.org/10.1186/s42408-023-00189-0>